Universitat de les Illes Balears

MASTER'S THESIS

EFFECTS OF A PALMITIC ACID AND FRUCTOSE-RICH DIET ON LUNG FIBROSIS AND INFLAMMATION MARKERS IN AGED MICE

Kristiyan Stiliyanov Atanasov

Master's Degree in Biomedical Research

(Translational)

Centre for Postgraduate Studies

Academic Year 2021-22

Effects of a palmitic acid and fructose-rich diet on lung fibrosis and inflammation markers in aged mice

Kristiyan Stiliyanov Atanasov

Master's Thesis

Centre for Postgraduate Studies

University of the Balearic Islands

Academic Year 2021-22

Key words:

Pulmonary fibrosis, idiopathic pulmonary fibrosis, palm oil, palmitic acid, fructose, age.

Thesis Supervisor's Name: Josep Mercader Barceló, Ernest Sala Llinàs

Index

ABSTRACT

Palmitic acid- and fructose-rich (PAF) diet could exert proinflammatory and profibrotic effects on aged mice. Bleomycin-induced lung injury could be exacerbated by PAF diet. PAF diet might contribute to proinflammatory and profibrotic lung reprogramming due to palmitic acid effect on lipid lung metabolism and TLR4 interaction and/or insulin resistance induced by fructose overload. Bleomycin-treated aged Swiss CD-1 mice showed increased extracellular matrix protein mRNA expression (Col1a1, Fn1) and PAF-fed bleomycin-treated mice showed higher overall expression levels. Untreated aged mice showed increased Fn1 expression and higher lymphocyte infiltration in airways in comparison with adult mice. Chronic exposure to PAF diet on adult, and specially aged mice, led to a proinflammatory lung state characterised by Il6 upregulation and cellular infiltration in airways and bronchoalveolar lavage fluid. To conclude, PAF diet exacerbates BLM-induced lung injury in aged mice and long-term exposure exerts a proinflammatory effect in lungs *per se*.

INTRODUCTION

Palm oil consumption has increased along the years with the addition as flavour enhancer in processed foods, which along the increase of the incidence of cardiovascular disease and obesity among the western population [1] has raised questions suggesting a potential detrimental effect of high PA consumption on health. PA is a 16 carbon saturated fatty acid (FA) (16:0) and the most abundant saturated fatty acid (SFA) on plant-derived fats. It is the main SFA in palm oil (85%), an oil extracted from the mesocarp of the oil palm plant (*Elaeis guineensis*) containing a balance of 48% saturated FAs (PA, stearic, lauric and myristic acid) and 52% unsaturated FAs (oleic and linoleic acid)[2]. Several animal studies have observed contrasting effects of PA on disease, ranging from a proinflammatory and profibrotic effect on liver [3] to an ameliorating effect on ischaemia-reperfusion injury by reducing the effect of reactive oxygen species (ROS)[4]. PA has also shown to alter glucose metabolism and homeostasis[5]. PA also can induce changes in lung dynamics, more specifically oxygen consumption[6], compared with oleic acid.

Idiopathic pulmonary fibrosis (IPF) is a chronic, progressive and fatal interstitial lung disease (ILD) with very limited therapeutic agents available and no curative therapy. IPF can be distinguished from other ILDs by the heterogeneity in fibrotic tissue formation, leading to a honeycomb pattern on MRI images. IPF has remained an orphan disease with no known cause although many risk factors and comorbidities have been associated with the disease. Common risk factors among lung diseases such as cigarette smoking or

particulate exposure have been defined as risk factor for IPF but other risk factors like age (the mean age of IPF patients being around 65 years)[7], diet and lung/gut microbiome have been also suggested[8]. Gastroesophageal reflux and diabetes mellitus type II are comorbidities in IPF patients, contributing to the idea of a role of nutrition and metabolism in IPF pathogenesis. The mechanism by which IPF is hypothesised to occur is the repetitive subclinical damage of the alveolar epithelium, promoting tissue remodelling: increased extracellular matrix (ECM) turnover, fibroblast hyperproliferation, leading to fibroblastic foci in lung parenchyma and fibroblast to myofibroblast differentiation [9]. Metabolic reprogramming of lung cells has also been suggested as a potential mechanism of pathogenesis[10].

Progressive fibrosing phenotype (PFP) is a recently identified phenotype of ILD patients characterised by rapid disease progression, leading to pronounced lung function decline with a subsequent decline of average quality of life and mortality increase in these patients [11]. The discovery of new risk factors for PFP development can help in improving disease outcome and early diagnosis [12].

The most common animal model for IPF and other ILDs is the intratracheal (i.t.) instillation of mice with a damaging agent, most commonly bleomycin (BLM), inducing lung epithelium damage leading to pulmonary fibrosis (PF). BLM-treated mice showcase many characteristics in common with IPF patients, such as fibroblastic activation, lung epithelial cell reprogramming but also differ greatly in the scarring pattern and progressiveness of the disease[13]. Another common point is the metabolic and lipidomic reprogramming in BLM-treated mice[14,15].

Lipidomic analysis of lung surfactant phospholipids in IPF patients have found increased levels of PA and stearic acid[16]. An epidemiologic studiy in a Japanese cohort of IPF patients found a positive correlation between saturated fat intake and IPF[17]. Elov16-deficient mice, a SFA metabolism enzyme, showed pulmonary fibrosis, suggesting an intrinsic role of SFA metabolism in PF pathogenesis[18]. Moreover, inhibitors of serine palmitoyl transferase (SPT), a protein palmitoyl group transferase, have been shown to ameliorate radiation-induced lung inflammation and fibrosis[19]. Lipidomic analysis of PPF patients and non-PPF IPF patients from an Australian cohort have found significant differences in lipid composition[20], suggesting a potential role of lung lipids in IPF progression and exacerbation.

SFA-rich diet promoted lung fibrosis in cockroach allergen-stimulated mice lungs and increased lung collagen in saline-instilled mice[21]. Long-term high fat diet exposure on mice induced lung fibrosis in a insulin resistance-mediated manner[22]. A

chicken fat-rich diet and 10% fructose supplementation induced lung upregulation of interleukin 6 (*Il6*) mRNA and incipient fibrosis[23]. PA-rich modified Western diet exposure contributed exacerbating BLM-induced lung fibrosis and upregulated ECM protein mRNA expression[16]. Stearic acid supplemented by oral gavage had a contrasting effect, ameliorating BLM-induced lung fibrosis[24], a phenomenon observed in cholestasis-induced liver fibrosis[25], suggesting a specificity of negative effects of SFAs on lung fibrosis (PA but not stearic acid).

HYPOTHESIS AND OBJECTIVE

Swiss CD-1 mice are an outbred wild-type mouse strain characterised by genetic heterogeneity that could better reproduce IPF features, given the polygenic nature of this disease. Age is an important risk factor in IPF development, therefore, aged mice might model IPF more accurately than young mice [13]. BLM-induced lung epithelium damage in association with age-related diminished wound healing capability might recapitulate human disease.

PA-rich modified Western diet containing a 42% of kcal in fat in addition to 10% fructose supplemented in drink water (PAF) might exacerbate BLM-induced lung fibrosis when administered after BLM challenge, leading to a worse outcome. Aged mice, given the glucose homeostasis capability decline associated with age, might show a higher vulnerability to diet effect.

Long-term exposure to PAF diet might induce lung remodelling as well as profibrotic and proinflammatory reprogramming possibly in an insulin resistance-mediated manner. Aged mice might showcase a higher sensitivity to PAF diet exposure. PAF diet might exert a profibrotic effect on aged mice, leading to incipient fibrosis *per se*, comparable to BLM-induced lung remodelling in adult mice.

Thus, the objective of this study is to evaluate the effect of PAF diet on the progression and development of PF using aged Swiss CD-1 mice.

EXPERIMENTAL DESIGN

Effects of different BLM dose were assessed to determine the optimal dose for PF modelling in Swiss CD-1 strain mice based on ECM protein and proinflammatory cytokine mRNA expression, as well as lung fibrosis Ashcroft score. Adult Swiss CD-1 female mice were subjected to i.t. BLM instillation of 3 different doses (2 U/kg, 6 U/kg or 12 U/kg) or phosphate buffer saline (PBS). After 2 weeks mice were sacrificed by CO_2 chamber (fig. 1A) and lung samples were collected for molecular determinations (mRNA levels by RT-qPCR) and histology (Ashcroft score) were taken *post mortem*.

To analyse the effect of PAF diet on BLM lung damage, aged (18 months) Swiss CD-1 female mice were i.t. instilled with 6 U/kg of BLM or PBS and subjected to PAF diet or

standard chow (SC) for 2 weeks before sacrifice. Body weight was measured to determine if PAF diet led to weight increase or the potential effect of BLM on aged mice weight. Lung samples were taken for molecular determinations (mRNA levels by RT-qPCR and protein levels by western blot), bronchoalveolar lavage fluid (BALF) was taken for cytological analysis by flow cytometry and lung samples were taken for histological determinations (Hematoxylin-Eosin and Sirius Red collagen staining).

To analyse the effect of PAF diet on the lungs *per se*, aged (18 months) and adult (4-6 months) female Swiss CD-1 mice were subjected to a 9-week exposure to PAF diet or SC. Body weight was measured throughout the experimental procedure to observe potential increase due to PAF diet. An independent group of adult female mice were i.t. instilled with 6 U/kg of BLM 2 weeks prior sacrifice. Endpoint glycaemia was measured following an 8-hour fast to elucidate whether insulin resistance was established and its potential role in PF. Lung samples were taken for molecular determinations (mRNA levels by RT-qPCR and protein levels by western blot), bronchoalveolar lavage fluid (BALF) was taken for cytological analysis by flow cytometry and lung samples were taken for histological determinations (Ashcroft score, Hematoxylin-Eosin and Sirius Red collagen staining). The effect of long-term PAF diet exposure on mice lungs, and the potential age-associated difference of response was assessed, while comparing with an experimental PF group to further characterise potential incipient fibrosis.

MATERIALS AND METHODS

Mice and Diet

Female Swiss CD1 mice of two different ages (aged mice, 18 months old, and adult mice, 2 to 6 months old) were divided in the aforementioned groups (see Experimental design section). Mice were caged in plexiglass ventilated cages with 5 to 6 individuals per cage following a 12-h light-dark cycle. Mice were fed two different dietary regimes: *ad libitum* fed Modified Western diet with Palm Oil 42% kcal Fat (TD.160620, Teklad Custom diet, Envigo) and 10% fructose (D(-)-fructose (USP, BP, Ph. Eur.) pure, pharma grade, ITW Reagents Panreac AppliChem) solution (PAF); and *ad libitum* standard chow 6% fat and filtered tap water (SC). Control of the weight and health of mice was kept once or twice a week. Mice were sacrificed by CO_2 chamber and tissue samples were taken by *post mortem* open thoracotomy.

Bleomycin administration

2 U, 6 U or 12 U of bleomycin (1.5 U = 1 mg)(bleomycin sulphate, MedChem Express) per kg of body weight dissolved in sterile PBS (Dulbecco Phosphate Buffer 1X, Bioline) were i.t. instilled following the method described by de Francisco, T et. al. [26] . Mice were sacrificed 14 days following instillation.

Glycaemia assessment

Tail vein blood glucose was measured following 8-h fast with a glucometer (GlucoChek, Aktivmed) and strips following tail vein cut using a few drops of blood.

RNA extraction

RNA was extracted from the right lung of mice after animal sacrifice. PBS washed lungs were snap-frozen in liquid nitrogen and stored at -80˚C. Total RNA extraction was performed by phenol-chloroform modified protocol using TRItidy commercial triple reagent. Resulting RNA precipitate was resuspended in 40 µl RNAse free water.

mRNA expression of fibrosis and inflammatory genes

Expression of key fibrosis and inflammatory genes was measured by real time semiquantitative polymerase chain reaction in the right lung lobes. cDNA, DNA primers, SYBR no ROX solution (SensiFAST™ SYBR® No-ROX Kit, Meridian Biosciences), DNA polymerase, desoxinucleotides (dNTPs) and SYBR Green nucleic acid fluorescent dye were mixed and pippeted in 96 well skirted qPCR plates. Analysis of Cycle threshold and melting curve was performed on a Bio-Rad CFX Real Time thermal cycler, performing a total of 40 cycles/run using commercially specified protocol for the qPCR Master mix. Primer sequences are detailed on Supplementary material 1.

Protein expression of fibrosis associated genes

Analysis of gene expression at the protein level was performed by western blot. Briefly, total protein extraction was performed by phenol-chloroform protocol taking the organic phase following TRItidy commercial protocol. The resulting extracts were quantified using a bicinchoninic acid (BCA) method-based commercial kit (Pierce™ BCA Protein Assay, ThermoFisher Scientific). Samples were prepared for SDS-PAGE loading 10 µg of total protein/sample according to Laemmli, et. al (Laemmli). Samples were loaded on 7% polyacrylamide gels with SDS and electrophoresis was carried out in a vertical cell. Protein transfer on a 0.45 µm pore PVDF membrane was performed using a semi-dry transfer method via TransBlot TURBO (BIO-RAD) transfer station with a custom protocol of 40 min at 22 V and 1.2 A. Membranes were blocked in blocking buffer* (5% BSA, Tween -20 0.1% and 0.05% sodium azide in TBS). Incubations with antibodies were performed o/n at 4˚C. Secondary antibody incubation was performed at RT during 1 h when needed. For membrane development a commercial ECL substrate was used (SuperSignal™ West Dura Extended Duration Substrate, ThermoFisher Scientific, 34075). Signal densitometry values were measured by chemoluminiscence on LAS 100 (GE Healthcare) and resulting bands were quantified with ImageStudio (Li-COR) image analysis software. Antibody dilution and

further information is on Supplementary material 2.

Flow cytometry of bronchoalveolar lavage fluid (BALF)

BALF was collected after injecting twice a 500 µl volume of sterile PBS into the lungs of mice following tracheotomy via a flexible cannula. Samples were centrifuged until cell pellet was visible. Cell pellet was resuspended in lysis buffers. 200 µl were used for flow cytometry using a BD FACSVerse (BD Biosciences) cytometer. Gating of lymphocyte, macrophage and granulocyte population was performed according to bibliography.

Histology of lung tissue

The right lung lobes of mice were cleaned via intracardiac punction with sterile saline solution to prevent blood clots in lung sections. Lungs were filled with 4% paraformaldehyde (PFA) until full inspiration volume. A ligature was performed to close the airways and the lungs were fixated in 4% PFA for 24 h. Fixed lungs were included in paraffin. Sections of paraffin embedded lungs were cut at 2 different thicknesses (5 µm for Sirius Red collagen staining, 4 µm otherwise) using a Leica microtome.

Sirius Red collagen staining

Sections were deparaffined by warming up slides at 35˚C for 5 min and washing in xylene for 5 min. Slides were rehydrated in concentration decreasing ethanol-water solutions (100%, 96%, 90% and 70% ethanol) for 5 min in each. A short wash with tap water before submerging in 1% phosphomolybdic acid for 2 min. Quicky wash with distilled water thrice and incubate slides in a solution of 0.1% Direct Red in saturated Picric acid for 1 hour. Slides were washed with 0.01N HCl for 2 min and dehydrate with the same water-ethanol solutions in reverse order 5 min in each. Incubate slides in xylene for 10 min and mount with DPX mounting medium.

Masson's Trichrome and Hematoxylin-Eosin staining

Masson's Trichrome staining was performed with the aid of automated staining devices following standard protocols.

Ashcroft score

Lung slides were scored according to the modified Ashcroft score (Ashcroft article) by a qualified pathologist.

Image analysis

Stained slides were observed with an inverted brightfield microscope (ZEISS AxioScan, Carl Zeiss) with a visible light/RGB camera ERc5S (Carl Zeiss). Sirius Red collagen airway deposition analysis was performed on 200x magnification images of Sirius Red stained slides with ImageJ software (ImageJ citation). H-E and Masson's trichrome stained slides images were taken using 50x and 100x magnification.

Statistical analysis

Results are represented as mean ± SEM. P < 0.05 was considered statistically significant (*). Data was analysed using Microsoft Excel 9.0 (Microsoft) software and GraphPad Prism 7 (Prism) software. To compare 2-factor defined groups Two-Way ANOVA followed by Bonferroni multiple comparisons *post hoc* test were used. For single factor comparation unpaired T test or One-Way ANOVA, depending on group number. Data distribution was analysed for normality using Kolmogorov-Smirnov test. Survival was assessed using Martel-Cox logrank test.

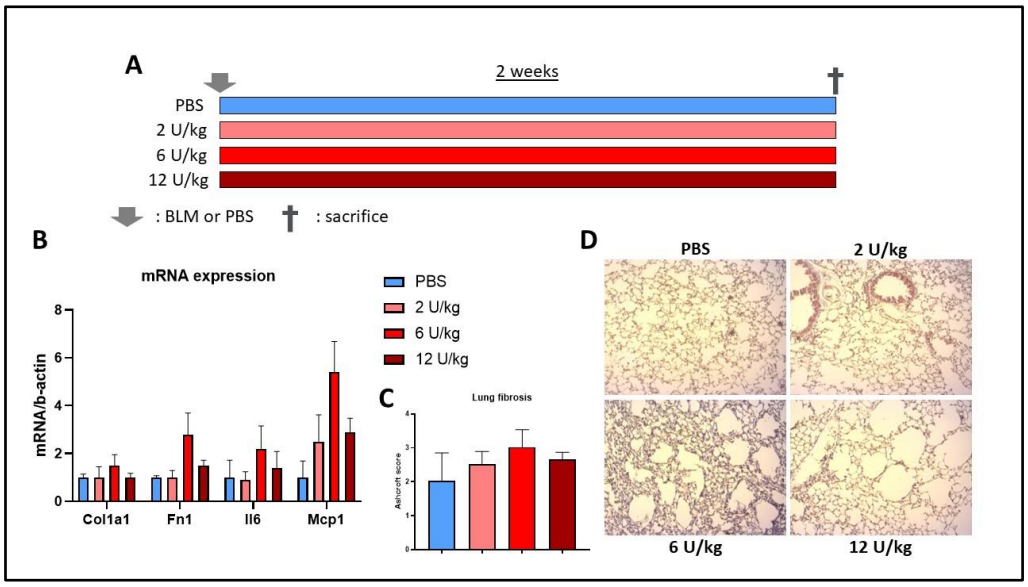

Figure 1. A. Experimental design of BLM dose experiment, consisting of i.t.instillation of PBS or BLM at three different doses (2 U/kg, 6 U/kg and 12 U/kg) and 2-week observation before sacrifice. B. mRNA levels normalised with *b-actin* mRNA of *Col1a1*, *Fn1, Il6* and *Mcp1*, represented as mean ± SEM. ANOVA one-way…C,. Ashcroft score for lung fibrosis on MT-stained lung sections. MT-stained sections showing apparent lung parenchymal thickening in 6 U/kg BLM-treated mice without architectural alterations or emphysema and PBS-instilled mice unaltered lung architecture.

RESULTS

6 U/kg BLM dose induced the highest lung damage in Swiss CD-1 mice

Swiss CD-1 adult female mice were challenged with three BLM doses to assess which one induces the maximum response (fig 1A). Mice showed the highest profibrotic (Col1a1, Fn1) and proinflammatory (Il6, Mcp1) (fig. 1B) gene expression when instilled with 6 U/kg BLM, gaining a 1.5-fold and 2.8-fold, for Col1a1 (P>0.05) and Fn1 (P=0.0985) respectively, and a 2.2- and 5.4-fold for Il6 (P>0.05) and Mcp1 (P=0.073). Ashcroft lung fibrosis score followed a similar trend as Fn1 expression being the highest (3.04±0.51) for 6 U/kg BLM-treated mice (fig. 1C), confirmed by moderate-to-high lung parenchyma thickening as in MT images (fig 1D).

BLM administration did not alter survival of aged mice

Final survival of BLM-treated SC-fed mice was 100%, as well as for BLM-treated PAF-

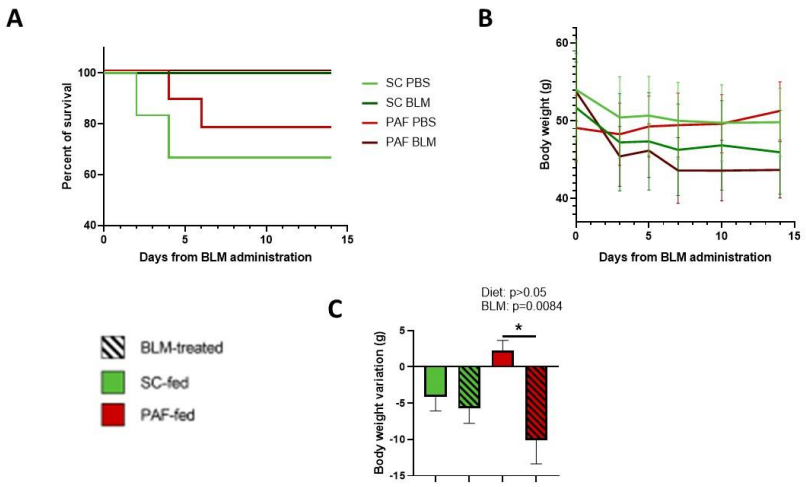

Figure 2. A. Survival of aged Swiss CD-1 female mice subjected to BLM challenge and/or 2-week PAF diet. B. Body weight (g) of aged mice subjected to BLM challenge and/or 2-week PAF diet. C. Body weight gain (g) (BWd14-BWd0). BLM-treated mice showed significant and progressive weight loss (2-Way ANOVA, 'BLM' p=0.0084).

fed mice after completing the intervention. For PBS-instilled SC-fed aged mice survival was 83,3% at day 2 and 66,6% at day 4 after instillation procedure. For PBS-instilled PAF-fed aged mice survival at day 4 was 88,9% and at day 6 was 77,8%. Martel-Cox logrank survival test did not show any significant differences among groups (X^2=4.527; p=0.2099). (fig. 2A)

BLM challenge reduced body weight in a diet independent manner in aged mice

Body weight reduction is a common marker for assessment of BLM-induced lung damage in the more widely used C57BL/6 mice strain. Here, we assessed BLM effect on body weight in the Swiss CD-1 strain Initial mean body weight among BLM and PBS-treated aged mice was not significantly different (p>0.05) (fig. 2B). _Mean BLM-treated aged mice body weight did not differ from PBS-instilled aged mice weight throughout the study (fig. 2B), but BLM-treated mice show a trend towards lower body weight. In contrast, at the end of the study, body weight gain was significantly reduced by BLM (p=0.0084) (fig. 2C). 2-week PAF diet exposure did not exert any significant effect on neither body weight nor body weight gain in aged mice (p>0.05). (fig. 2B and C).

BLM-treated aged mice showed increased lung Il6 and Mcp1 mRNA levels but not Il1β

BLM challenge induced Il6 (p=0.0290) (fig. 3A) and Mcp1 (p=0.0467) mRNA expression (fig. 3B) when compared with PBS-instilled mice. SC-fed aged mice showed a 1.5-fold increase for Il6 mRNA and 2-fold for Mcp1, while PAF-fed aged mice showed a more marked induction with a 10-fold increase for Il6 and 6.5-fold increase for Mcp1. Il1β mRNA levels were unchanged by

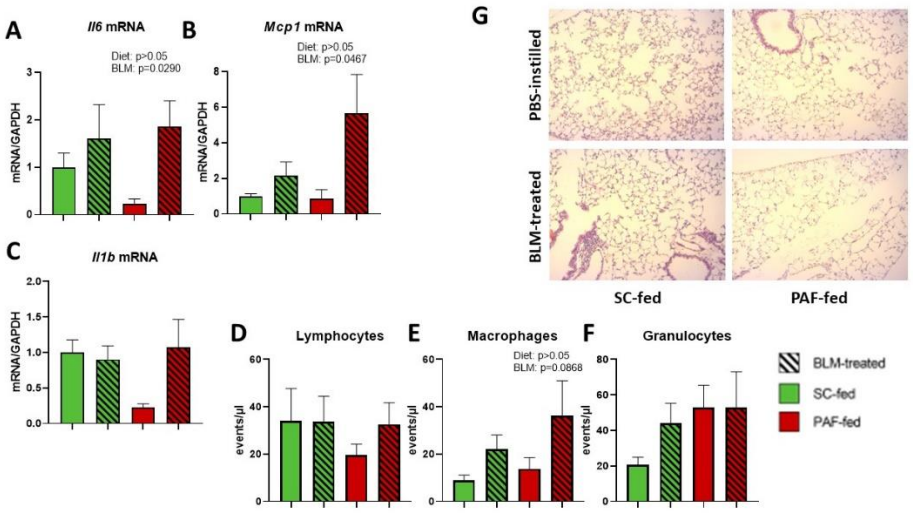

Figure 3. A. Lung *Il6* mRNA expression, BLM-treated aged mice showcased increased *Il6* mRNA than PBS-instilled (2-Way ANOVA, 'BLM' p=0.0290). B. Lung *Mcp1* mRNA levels, BLM challenge increased *Mcp1* levels (2-Way ANOVA, 'BLM' p=0.0467) in aged mice. C. *Il1*β mRNA levels. D, E and F. Flow cytometry of BALF, lymphocyte (D), macrophage (E) and granulocyte (F) count. Macrophages showed a trend towards increase (2-Way ANOVA, 'BLM' p=0.0868) in response to BLM challenge in aged mice. G. H&E-stained lung sections at 100x magnification. BLM-treated PAF-fed mice showed regions of diffusely distributed macrophage accumulation (bottom right).

BLM challenge alone (p>0.05) but interaction between 2-week PAF diet exposure and BLM challenge resulted in a trend towards increase (p=0.0924) in PAF-fed mice (fig. 3C).

BLM challenge showed a trend to increase macrophage cell count in aged mice airways

BALF macrophage count was 2.5 and 2.6 -fold increase in SC-fed and PAF-fed mice, respectively, which did not reach statistical signicance (p=0.0868) (fig. 3D). PAF-fed BLM-treated mice showed regions of macrophage accumulation diffusely distributed along the latero-basal and basal segments of lower lobes (fig. 3G) Lymphocyte count (fig. 3E) and granulocyte count (fig. 3F) were unaltered in response to BLM challenge in aged mice (p>0.05), but lymphocyte infiltration foci could be identified on perivascular-peribronchial junctions on both SC-fed and PAF-fed BLM-treated mice (fig. 3G), suggesting acute phase inflammation in airways. 2-week PAF diet exposure did not result in altered immune cell (macrophages, lymphocyte and granulocyte) count in BALF, although granulocytes had overall higher cell count in PAF-fed mice BALF.

ECM proteins mRNA levels were more markedly increased by BLM challenge in PAF-fed mice

BLM-treated aged mice showed increased lung *Col1a1* (p=0.0458) (fig. 4A) and *Fn1* (p=0.0134) (fig. 4B) mRNA levels, suggesting an increase in ECM protein expression. 2-

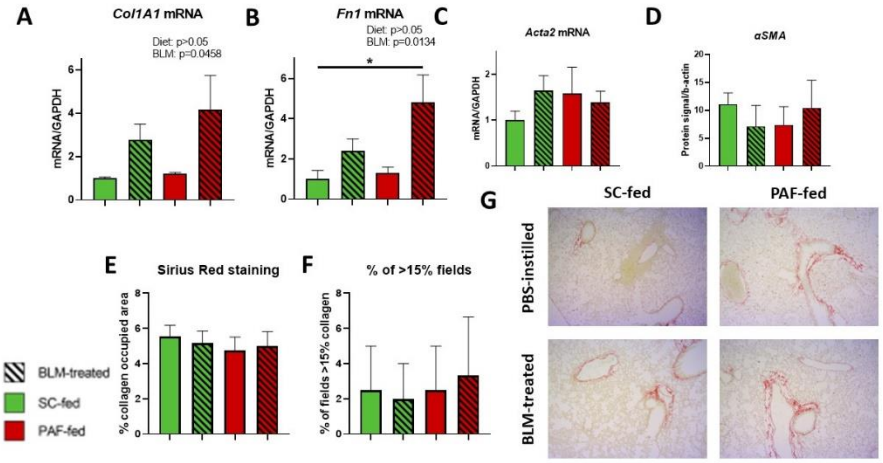

Figure 4. A. *Col1a1* mRNA expression in mice lungs. BLM challenge increased *Col1a1* mRNA levels (2-Way ANOVA, 'BLM' p=0.0458) in aged mice. B. *Fn1* mRNA expression in mice lungs. BLM-treated aged mice showcased increased *Fn1* mRNA than untreated mice (2-Way ANOVA, 'BLM' p=0.0134), which only comparing SC-fed untreated mice with 2-week PAF diet exposed BLM-treated mice was significant (*post hoc* Bonferroni Multiple comparisons *p=0.0306). C, D. *Acta2* mRNA (C) and protein (D) levels. E, F and G. Sirius Red collagen staining of lung slides for collagen deposition around airways.

week PAF diet exposure on aged mice did not alter *Col1a1* or *Fn1* mRNA levels (fig. 4A and B), but BLM increased *Col1a1* mRNA 2.4-fold in SC-fed mice and 3.5-fold in PAF-fed mice, while *Fn1* mRNA was increased in response to BLM 2.3-fold in SC-fed mice and 3.7-fold in PAF-fed mice, suggesting a potential synergy.

Alpha smooth muscle actin mRNA and protein levels were unchanged in response to BLM challenge and/or 2-week PAF diet exposure in aged mice

Alpha smooth muscle actin (αSMA) lung mRNA (Acta2) and protein levels were unaltered in BLM-treated aged mice (p>0.05). 2-week PAF diet exposure did not exert any effects on Acta2 mRNA and αSMA protein levels (p>0.05 for both) (figure 4C and D).

Airway collagen deposition was unchanged in response to BLM challenge or 2-week PAF diet exposure in Swiss CD-1 aged mice

Percentage of collagen occupied area around airways was not increased in response to BLM challenge (p>0.05), in neither SC-fed nor PAF-fed aged mice. 2-week PAF diet exposure did not affect collagen deposition around airways (p>0.05) (figure 4E, F and G).

Chronic PAF diet exposure did not exert any effect on survival

Survival was unaltered by BLM challenge in adult mice. Chronically PAF-fed mice, both

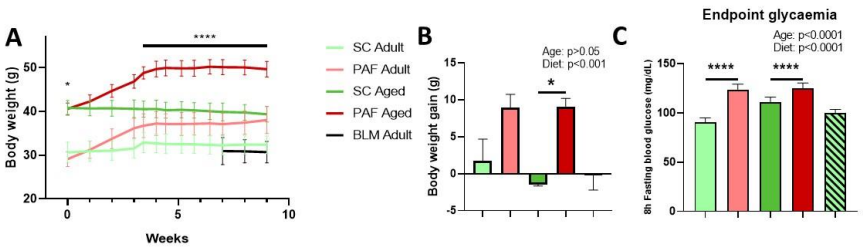

Figure 5. A. Body weight (g) was increased in response to chronic exposure to PAF diet (**** p<0.0001) in both adult and aged mice, while aged mice showed higher initial body weight values (* p=0.0120). While weight increase was observed in chronic PAF diet exposed mice aged mice had a higher body weight overall (**** p<0.0001) and the increase due to PAF diet was more pronounced. B. Body weight change (g) was highly positive for chronic PAF diet exposed mice but barely positive for SC-fed mice (p<0.0001), aged mice showed greatest PAF diet associated difference (*p=0.0231). C. Fasting glycaemia (mg/dl) was increased (*p=0.0012) after chronic PAF diet. Aged mice showed higher endpoint fasting glycaemia (p<0.0001) than adult mice.

adult and aged, survived until the end of the experimental procedure.

Chronic PAF diet exposure increased body weight in adult, and more markedly in aged mice.

BLM-treated adult mice did not show a significant reduction in body weight (p>0.05) (fig. 5A). Chronic PAF diet exposure resulted in a body weight increase from day 24 and throughout the study (p<0.0001) in adult (p=0.0153), and more markedly, in aged mice (p<0.0001) (fig. 5A). End-point body weight was increased 1.2-fold for adult mice chronically exposed to PAF diet and 1.3-fold for aged mice. Body weight gain was positive for PAF-fed mice but negative for SC-fed mice (p<0.0001) (fig. 5B), having a more marked change in PAF-fed aged mice (p=0.0006) than PAF-fed adult mice (p=0.0603).

Glycaemia was increased in chronically PAF-fed mice but remained within normal levels.

Bleomycin did not exert any significant effect on fasting glycaemia (p>0.05) (fig. 5C). Chronic PAF diet exposure increased endpoint glycaemia (p=0.0012) in both adult and aged PAF-fed mice (p<0.0001 for both) (fig. 5C). Regardless of PAF diet effect, glucose homeostasis was not altered (endpoint fasting glycaemia<140 mg/dL). SC-fed aged mice showcased increased endpoint glycaemia in comparison with their adult counterparts (p<0.0001) (fig. 5C).

Chronic PAF diet exposure increased lung Il6 mRNA levels

BLM challenge did not increase proinflammatory cytokine (Il6, Il1β, Mcp1 and Tnfα) mRNA levels (p>0.05) in adult mice (fig. 6A-D).

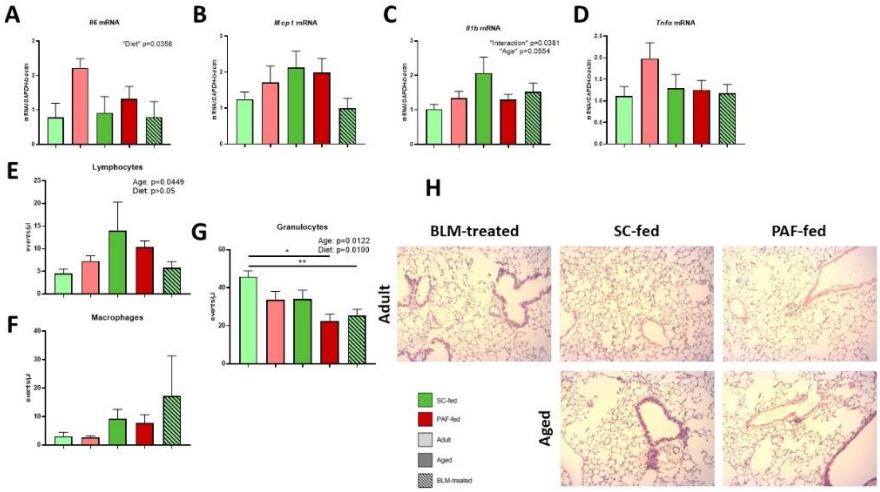

Figure 6. A, B, C and D. *Il6*, *Mcp1*, *Il1β* and *Tnfα* mRNA levels as measured by RT-qPCR. BLM challenge in adult mice did not increase proinflammatory cytokine mRNA levels. Chronic PAF diet exposure increased (p=0.0358) *Il6* mRNA levels. Aged mice showed a trend towards *Il1*β mRNA levels increase (p=0.0554) which became a significant increase with the interaction of chronic PAF diet exposure (p=0.0381). E, F and G. BALF lymphocytes, macrophages and granulocytes, respectively). Chronic PAF diet exposure decreased granulocyte count (events/µl) (p=0.0100). Aged mice showed increased lymphocyte count (p=0.0449) and an increasing trend for macrophage count (p=0.0621). H. H&E-stained lung sections at a 100x magnification. BLM-treated adult mice lungs showcase airway macrophage accumulation and lung epithelial cell metaplasia. Aged mice show perivascular (right image) and peribronchial (left image) lymphocyte infiltration, slightly attenuated in PAF-fed mice.

Chronic PAF diet exposure increased lung Il6 mRNA levels (p=0.0358) (fig. 6A) but did not exert any significant effects on other proinflammatory cytokine mRNA levels (fig. 6B-D). Aged mice did show a trend towards an increase of Il1β mRNA levels (p=0.0554) which in interaction with chronic PAF diet exposure gained significance (p=0.0381) (fig. 6C).

Chronic PAF diet exposure decreased granulocyte cell count in BALF.

BLM-treated adult mice did not show any differences in immune cell populations in BALF when compared with untreated mice (p>0.05) (fig. 6E-G). Chronic PAF diet exposed mice showed decreased granulocyte count in BALF compared with SC-fed mice (p=0.0100) (fig. 6F). Lymphocyte and macrophage count were unchanged in response to chronic PAF diet exposure (p>0.05) (fig. 6E, G). Aged mice suffered a general change in immune cell populations in BALF (fig. 6E-G). Lymphocytes were increased in aged mice BALF (p=0.0449) compared with adult mice. Moderate-to-severe lymphocytic infiltration occurred on perivascular and peribronchial zones of aged mice, being more pronounced in SC-fed mice than in PAF-fed mice (fig. 6H). Moreover, macrophage count also showed a trend towards an increase in aged mice (p=0.0621) and macrophage accumulation could be observed

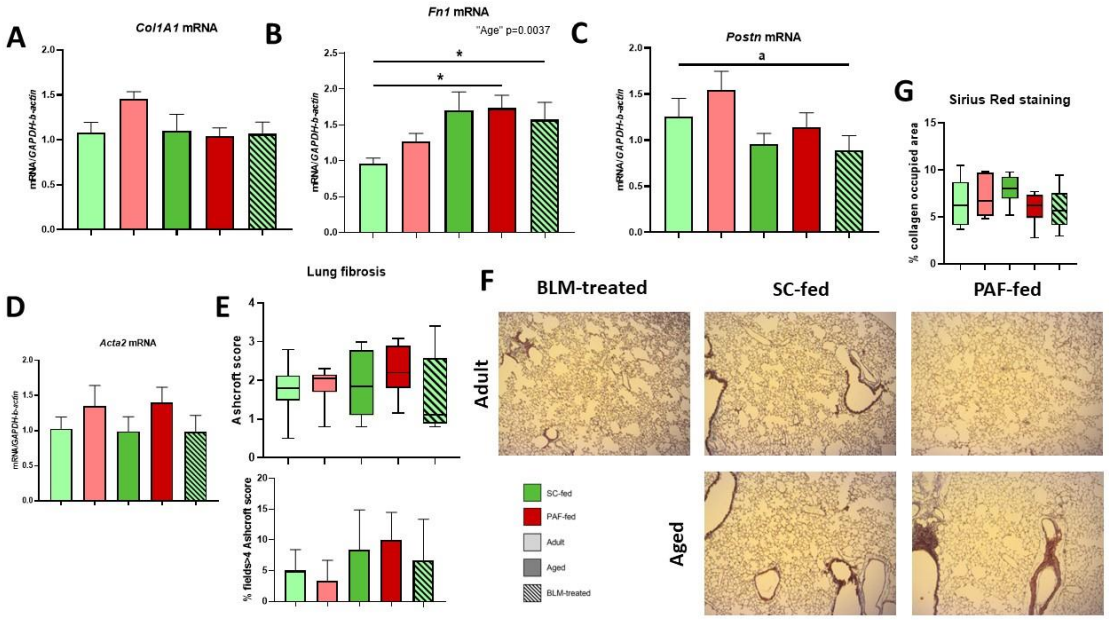

Figure 7. A. *Col1a1* mRNA levels measured by RT-qPCR. B. *Fn1* mRNA levels as measured by RT-qPCR. BLM-treated adult mice showed increased Fn1 mRNA levels (Student T-test, p=0.0361). Aged mice showcased increased *Fn1* mRNA levels (2-Way ANOVA, 'Age' p=0.0037). C. *Postn* mRNA levels as measured by RT-qPCR, a trend to decrease was observed in BLM-treated adult mice ('a': Student T test, p=0.0824). Aged mice showed a trend towards a decrease (2-Way ANOVA, 'Age' p=0.0625) in Postn mRNA levels. D. *Acta2* mRNA as measured by RT-qPCR. E, F. Ashcroft score of MT-stained lung slides. 50x magnification MT-stained lung sections. BLM-treated adult mice lungs showcase denser parenchyma and altered tissue architecture. PAF-fed aged mice lungs showcase some collagen deposition and perivascular-peribronchial junction lymphocytic infiltration (top left of micrograph). G. Sirius Red collagen staining and collagen deposition quantification around airways.

in smaller airways (alveoli and bronchial-alveolar junctions) (fig. 6H). Granulocyte count, as with chronic PAF diet exposure, was decreased in aged mice (p=0.0122).

Fn1 mRNA levels in PAF-fed aged mice were as high as those induced by BLM

While Col1a1 mRNA levels were not induced by BLM (fig. 7A), BLM-treated adult mice showed higher Fn1 mRNA levels than untreated adult mice (p=0.0361) (fig. 7B). Chronic PAF diet exposure did not affect significantly mRNA levels of ECM proteins (p>0.05 for both Fn1 and Col1a1) (fig. 7A-B). Aged mice showcased increased Fn1 mRNA levels (p=0.0037) (fig. 7B), which in the case of PAF-fed aged mice did not differ from BLM-treated adult mice (p>0.05). Periostin (Postn), another ECM protein, showed a decreasing trend for aged mice (p=0.0625) as well as BLM-treated adult mice (p=0.0824) (fig. 7C).

αSMA mRNA and protein levels were unaltered in response to chronic PAF diet exposure or BLM challenge

Acta2 mRNA levels were unaltered in BLM-treated adult mice (p>0.05). Neither chronic PAF diet exposure nor age showed any effect on αSMA expression (Acta2 mRNA levels) (fig. 7D).

Chronic PAF diet exposure did not induce fibrosis in adult or aged mice

Ashcroft score of BLM-treated adult mice was not significantly higher than untreated adult mice ($p>0.05$) and average score (1.6) (fig. 7E, F). Chronic PAF diet exposure did not have any significant effect on Ashcroft score, but PAF-fed aged mice did showcase the highest average score (2.2) and some collagen deposition with perivascular-peribronchial junction lymphocytic infiltration was observed (fig. 7E).

Collagen deposition was unaltered by BLM challenge in adult mice or by chronic PAF diet exposure in adult and aged mice

BLM challenge did not alter collagen deposition around airways in adult mice lungs ($p>0.05$) according to Sirius Red staining (fig. 7G). Chronic PAF diet exposure did not result in any significant change in collagen deposition ($p>0.05$) (fig. 7G). Aged mice did not show an increased collagen deposition in lungs ($p>0.05$) (fig. 7G).

Chronic PAF diet exposure did not increase Phospho (Ser109)-mammalian target of rapamycin (p-mTOR) levels significantly

BLM challenge did not result in p-mTOR levels change in adult mice ($p>0.05$). Chronic PAF diet exposure did not increase significantly p-mTOR levels ($p>0.05$) but did result in considerable quantitative increase in chronically PAF-fed aged (260-fold) and especially adult mice (300-fold) (fig. 8). Aged mice also showed increased average p-mTOR levels compared with SC-fed adult mice, but no significant difference ($p>0.05$) (Supplementary material, fig. 2).

DISCUSSION

6 U/kg of BLM IT-instilled did not induce PF development (based on Ashcroft score) in adult Swiss CD-1 mice but lower doses (2 U/kg) are able to induce PF in C57BL6 mice, which suggests an intrinsic resistance to BLM-induced damage in mice of this genetic lineage [27]. This phenomenon could be attributed to genetic heterogeneity in Swiss CD-1 outbred mice against the genetic homogeneity in other commonly used inbred strains. Moreover, other commonly observed characteristics of BLM-induced PF were not present in BLM-treated adult Swiss CD-1 mice like increased mortality or body weight decline. On the other hand, aged Swiss CD-1 mice did show an increase in ECM protein mRNA expression, as well as a trend in body weight decline, possibly suggesting the use of aged mice as a better model for IPF. Aged mice treated with BLM are very interesting as a model for IPF and PPF due to the intrinsic decline in wound healing function associated with age [28]and the localized action of i.t. instilled BLM, generating lung epithelium remodelling, as in IPF. BLM-treated aged mice subjected to a 2-week PAF diet exposure did not showcase increased ECM protein mRNA expression in comparison with SC-fed BLM-treated mice, which suggests that in a short period protocol, as in BLM-induced PF, PAF diet did not alter significantly PF outcome.

PA has shown to exert a proinflammatory effect in diseases like chronic kidney disease

or DMTII, modifying inflammatory cytokine and chemokine transcriptional profile and promoting immune cell infiltration[2]. In the case of DMTII and liver disease, SFAs can act as a profibrotic stimulus. In the case of long-term exposure to PAF diet, lung mRNA expression of Il6 was increased in both adult and aged mice but mice were not insulin resistant, suggesting an insulin-independent effect of PAF diet in the lungs, in contrast to other studies[22,23], these data are backed by in vitro studies proving an alternative insulin-independent mechanism of cytokine upregulation in mice pneumocytes[16]. A potential pathway by which PA might exert an effect is the activation of Toll-like receptor 4 by ligand-receptor interaction with PA, as it has been confirmed to possess the function of TLR4 ligand[29]. Our initial notion of mTOR-mediated action of PA on lungs was inconclusive but studies have shown antifibrotic effects of mTOR inhibitors on experimental PF[30].

Cellular inflammation in lungs of HFD-fed mice was characterised by lower granulocyte (more specifically eosinophil) and lymphocyte count than SC-fed mice [21], which matched PAF-fed mice BALF cell alterations. In contrast, chicken fat-rich diet and fructose fed mice showed increased lymphocyte count [23].

CONCLUSIONS

Swiss CD-1 mice show resistance to BLM-induced lung damage in comparison to other strains. BLM-treated aged mice show more signs of lung damage and tend to develop more IPF-like characteristics than adult mice. PAF diet might exacerbate BLM-induced lung injury, suggesting a role in PF progression. Chronic PAF diet generates a proinflammatory lung state *per se*, without triggering signs of lung fibrosis. The development of insulin resistance might be necessary to trigger lung fibrosis features.

REFERENCES

1. Ismail SR, Maarof SK, Ali SS, Ali A. Systematic review of palm oil consumption and the risk of cardiovascular disease. *PLoS ONE*. 2018;13(2):1-16. doi:10.1371/journal.pone.0193533
2. Gesteiro E, Guijarro L, Sánchez-Muniz FJ, et al. Palm oil on the edge. *Nutrients*. 2019;11(9):1-36. doi:10.3390/nu11092008
3. Mancini A, Imperlini E, Nigro E, et al. Biological and nutritional properties of palm oil and palmitic acid: Effects on health. *Molecules*. 2015;20(9):17339-17361. doi:10.3390/molecules200917339
4. Odia OJ. Palm oil and the heart: A review. *World Journal of Cardiology*. 2015;7(3):144. doi:10.4330/wjc.v7.i3.144
5. Zulkiply SH, Balasubramaniam V, Bakar NAA, Rashed AA, Ismail SR. Effects of palm oil consumption on biomarkers of glucose metabolism: A systematic review. *PLoS ONE*. 2019;14(8):1-14. doi:10.1371/journal.pone.0220877

6. Børsheim E, Kien CL, Pearl WM. Differential effects of dietary intake of palmitic acid and oleic acid on oxygen consumption during and after exercise. *Metabolism: Clinical and Experimental*. 2006;55(9):1215-1221. doi:10.1016/j.metabol.2006.05.005
7. Maher TM, Bendstrup E, Dron L, et al. Global incidence and prevalence of idiopathic pulmonary fibrosis. *Respiratory Research*. 2021;22(1):1-10. doi:10.1186/s12931-021-01791-z
8. Mercader-Barceló J, Truyols-Vives J, Río C, López-Safont N, Sala-Llinàs E, Chaplin A. Insights into the role of bioactive food ingredients and the microbiome in idiopathic pulmonary fibrosis. *International Journal of Molecular Sciences*. 2020;21(17):1-26. doi:10.3390/ijms21176051
9. Wynn TA. Integrating mechanisms of pulmonary fibrosis. *Journal of Experimental Medicine*. 2011;208(7):1339-1350. doi:10.1084/jem.20110551
10. Zhao H, Dennery PA, Yao H. Metabolic reprogramming in the pathogenesis of chronic lung diseases, including BPD, COPD, and pulmonary fibrosis. *American Journal of Physiology - Lung Cellular and Molecular Physiology*. 2018;314(4):L544-L554. doi:10.1152/ajplung.00521.2017
11. Cottin V, Hirani NA, Hotchkin DL, et al. Presentation, diagnosis and clinical course of the spectrum of progressive-fibrosing interstitial lung diseases. *European Respiratory Review*. 2018;27(150). doi:10.1183/16000617.0076-2018
12. Olson AL, Gifford AH, Inase N, Fernández Pérez ER, Suda T. The epidemiology of idiopathic pulmonary fibrosis and interstitial lung diseases at risk of a progressive-fibrosing phenotype. *European Respiratory Review*. 2018;27(150). doi:10.1183/16000617.0077-2018
13. Tashiro J, Rubio GA, Limper AH, et al. Exploring animal models that resemble idiopathic pulmonary fibrosis. *Frontiers in Medicine*. 2017;4(JUL):1-11. doi:10.3389/fmed.2017.00118
14. Weckerle J, Picart-Armada S, Klee S, et al. Mapping the metabolomic and lipidomic changes in the bleomycin model of pulmonary fibrosis in young and aged mice. *DMM Disease Models and Mechanisms*. 2022;15(1). doi:10.1242/dmm.049105
15. Hsu HS, Liu CC, Lin JH, et al. Involvement of ER stress, PI3K/AKT activation, and lung fibroblast proliferation in bleomycin-induced pulmonary fibrosis. *Scientific Reports*. 2017;7(1):1-11. doi:10.1038/s41598-017-14612-5
16. Chu SG, Villalba JA, Liang X, et al. Palmitic acid-rich high-fat diet exacerbates experimental pulmonary fibrosis by modulating endoplasmic reticulum stress. *American Journal of Respiratory Cell and Molecular Biology*. 2019;61(6):737-746. doi:10.1165/rcmb.2018-0324OC
17. Miyake Y, Sasaki S, Yokoyama T, et al. Dietary fat and meat intake and idiopathic pulmonary fibrosis: A case-control study in Japan. *International Journal of Tuberculosis and Lung Disease*. 2006;10(3):333-339.
18. Sunaga H, Matsui H, Ueno M, et al. Deranged fatty acid composition causes pulmonary fibrosis in Elovl6-deficient mice. *Nature Communications*. 2013;4. doi:10.1038/ncomms3563

19. Gorshkova I, Zhou T, Mathew B, et al. Inhibition of serine palmitoyltransferase delays the onset of radiation-induced pulmonary fibrosis through the negative regulation of sphingosine kinase-1 expression. *Journal of Lipid Research*. 2012;53(8):1553-1568. doi:10.1194/jlr.M026039
20. Nambiar S, Clynick B, How BS, et al. There is detectable variation in the lipidomic profile between stable and progressive patients with idiopathic pulmonary fibrosis (IPF). *Respiratory Research*. 2021;22(1):1-8. doi:10.1186/s12931-021-01682-3
21. Ge XN, Greenberg Y, Reza Hosseinkhani M, et al. High-fat diet promotes lung fibrosis and attenuates airway eosinophilia after exposure to cockroach allergen in mice. *Experimental Lung Research*. 2013;39(9):365-378. doi:10.3109/01902148.2013.829537
22. Park YH, Oh EY, Han H, et al. Insulin resistance mediates high-fat diet-induced pulmonary fibrosis and airway hyperresponsiveness through the TGF-β1 pathway. *Experimental and Molecular Medicine*. 2019;51(5). doi:10.1038/s12276-019-0258-7
23. Vedova MCD, Soler Garcia FM, Muñoz MD, et al. Diet-Induced Pulmonary Inflammation and Incipient Fibrosis in Mice: a Possible Role of Neutrophilic Inflammation. *Inflammation*. 2019;42(5):1886-1900. doi:10.1007/s10753-019-01051-9
24. Kim HS, Yoo HJ, Lee KM, et al. Stearic acid attenuates profibrotic signalling in idiopathic pulmonary fibrosis. *Respirology*. 2021;26(3):255-263. doi:10.1111/resp.13949
25. Pan PH, Lin SY, Ou YC, et al. Stearic acid attenuates cholestasis-induced liver injury. *Biochemical and Biophysical Research Communications*. 2010;391(3):1537-1542. doi:10.1016/j.bbrc.2009.12.119
26. de Francisco Casado MT, Mercader Barceló J and Rio Bocos C. Técnica ciega de administración intratraqueal de sustancias en ratones: simplificando la metodología. Animales de Laboratorio. Secal. 2022; 93 (1) 23-25.
27. Walkin L, Herrick SE, Summers A, et al. The role of mouse strain differences in the susceptibility to fibrosis: A systematic review. *Fibrogenesis and Tissue Repair*. 2013;6(1):1. doi:10.1186/1755-1536-6-18
28. He S, Sharpless NE. Review Senescence in Health and Disease. *Cell*. 2017;169(6):1000-1011. doi:10.1016/j.cell.2017.05.015
29. Dong Z, Zhuang Q, Ning M, Wu S, Lu L, Wan X. Palmitic acid stimulates NLRP3 inflammasome activation through TLR4-NF-κB signal pathway in hepatic stellate cells. *Annals of Translational Medicine*. 2020;8(5):168-168. doi:10.21037/atm.2020.02.21
30. Lawrence J, Nho R. The role of the mammalian target of rapamycin (mTOR) in pulmonary fibrosis. *International Journal of Molecular Sciences*. 2018;19(3). doi:10.3390/ijms19030778